Self-Assembled Fibrillar Networks through Highly Oriented Aggregates of Porphyrin and Pyrene Substituted by Dialkyl L-Glutamine in Organic Media†

Takashi Sagawa,*,‡ Sachiko Fukugawa,§ Taisuke Yamada,§ and Hirotaka Ihara*,§

Institute of Advanced Energy, Kyoto University, Gokasho, Uji 611-0011, Japan, and Department of Applied Chemistry & Biochemistry, Kumamoto University, 2-39-1 Kurokami, Kumamoto 860-8555, Japan

Received January 11, 2002. In Final Form: March 14, 2002

Microfibrous self-aggregation of chromophoric groups of porphyrin and/or pyrene substituted by didodecyl L-glutamic acid in organic media is confirmed by transmission electron microscopic (TEM) observation. Chromophoric probes of porphyrin and pyrene moieties enable evaluation of their assembling behavior photophysically through UV−vis, circular dichroism (CD), and fluorescence spectroscopic characterization. This spectroscopic characterization was able to compensate the lack of TEM observation for the aggregation even at a low concentration below the critical gel concentration. The temperature affects the salient features of the photophysics of porphyrin or pyrene in the microfibrous assemblies. Highly oriented network structures were formed at low temperature since the CD intensities of the porphyrin and pyrene systems increased with lowering the temperature. Fluorescence spectroscopic characterization confirmed the monomer excitation of porphyrin itself, and efficient excimer formation for the pyrene−pyrene charge transfer was detected at low temperature. In particular, we also obtained the preliminary results of fluorescence spectroscopic measurement on singlet−singlet energy migration from pyrene to porphyrin in the mixed assemblies for mimicry of the efficient energy transfer process of the photosynthetic antenna complex.

Introduction

Various kinds of low molecular weight compounds have been found to assemble in organic solvents in recent years.[1−25] Self-aggregation of these systems through intermolecular interactions such as hydrogen bonding, the solvophobic effect, and so on leads to the formation of fibrous networks in most cases. In the past decade, we have had a great interest in L-glutamic acid derived systems with three amide bonds as self-assembling materials.[18−25] The L-glutamic acid derived systems produce organic gels through formation of the self-aggregation by hydrogen bonding interaction among the amide moieties in organic solvents such as benzene, ethanol, cyclohexane, and so on. Formation of organic gels can be visually observed. However, we estimate that the L-glutamic acid derived compounds form aggregates even in the sol-forming concentration range, and so to evaluate the exact critical aggregation concentration (cac) is very important because the suprafunctions are probably brought about through molecular aggregation. We previously reported on the indirect detection of the aggregation structures of L-glutamic acid derived systems by a dye-complexation method.[24] In this paper, we studied the direct evaluation of an aggregation threshold prior to the sol−gel phase transition applied to newly synthesized protoporphyrin IX and/or pyrene substituted by dialkyl L-glutamine as a protoporphyrin IX 13,17-bis[*N*′,*N*′′-didodecyl-*N*-(2-aminopropionyl)- L-glutamide] (**1**) and pyrene-containing didodecylamide-type compound (**2**) in an organic solvent. Porphyrin and pyrene have been selected in this report since they are by far the most frequently used dyes in spectroscopic studies through UV−vis, circular dichroism (CD), and fluorescence character-

* Corresponding author. Telephone & Fax: +81-774-38-3511. E-mail: sagawa@iae.kyoto-u.ac.jp.

† This article is part of the special issue of *Langmuir* devoted to the emerging field of self-assembled fibrillar networks.

‡ Kyoto University.

§ Kumamoto University.

(1) Twieg, R. J.; Russell, T. P.; Siemens, R.; Rabolt, J. F. *Macromolecules* **1985**, *18*, 1361.
(2) Lin, Y. C.; Weiss, R. G. *Macromolecules* **1987**, *20*, 414.
(3) Scartazzini, R.; Luisi, P. L. *J. Phys. Chem.* **1988**, *92*, 829.
(4) Murata, K.; Aoki, M.; Nishi, T.; Ikeda, A.; Shinkai, S. *Chem. Commun.* **1991**, 1715.
(5) Hanabusa, K.; Okui, K.; Karaki, K.; Koyama, T.; Shirai, H. *Chem. Commun.* **1992**, 1371.
(6) de Vries, E. J.; Kellogg, R. M. *Chem. Commun.* **1993**, 238.
(7) Terech, P.; Weiss, R. G. *Chem. Rev.* **1997**, *97*, 3133.
(8) Hafkamp, R. J.; Kokke, B. P. A.; Danke, I. M.; Geurts, H. P. M.; Rowan, A. E.; Feiters, M. C.; Nolte, R. J. M. *Chem. Commun.* **1997**, 545.
(9) Garner, C. M.; Terech, P.; Allegraud, J. J.; Mistrot, B.; Nguyen, P.; de Geyer, A.; Rivera, D. *J. Chem. Soc., Faraday Trans.* **1998**, *94*, 2173.
(10) Tian, H. J.; Inoue, K.; Yoza, K.; Ishi-i, T.; Shinkai, S. *Chem. Lett.* **1998**, 871.
(11) Mizoshita, N.; Kutsuna, T.; Hanabusa, K.; Kato, T. *Chem. Commun.* **1999**, 781.
(12) Luo, X.; Li, C.; Liang, Y. *Chem. Commun.* **2000**, 2091.
(13) Jung, J. H.; Ono, Y.; Sakurai, K.; Sano, M.; Shinkai, S. *J. Am. Chem. Soc.* **2000**, *122*, 8648.
(14) Kimura, M.; Kitamura, T.; Muto, T.; Hanabusa, K.; Shirai, H.; Kobayashi, N. *Chem. Lett.* **2000**, 1088.
(15) Kölbel, M.; Menger, F. M. *Chem. Commun.* **2001**, 275.
(16) Partridge, K. S.; Smith, D. K.; Dykes, G. M.; McGrail, P. T. *Chem. Commun.* **2001**, 319.
(17) Luo, X.; Liu, B.; Liang, Y. *Chem. Commun.* **2001**, 1556.
(18) Ihara, H.; Hachisako, H.; Hirayama, C.; Yamada, K. *Chem. Commun.* **1992**, 1244.
(19) Takafuji, M.; Ihara, H.; Hirayama, C.; Hachisako, H.; Yamada, K. *Liq. Cryst.* **1995**, *18*, 97.
(20) Ihara, H.; Shudo, K.; Takafuji, M.; Hirayama, C.; Hachisako, H.; Yamada, K. *Kobunshi Ronbunshu* **1995**, *52*, 606.
(21) Ihara, H.; Shudo, K.; Hirayama, C.; Hachisako, H.; Yamada, K. *Liq. Cryst.* **1996**, *20*, 807.
(22) Hachisako, H.; Ihara, H.; Kamiya, T.; Hirayama, C.; Yamada, K. *Chem. Commun.* **1997**, 19.
(23) Hachisako, H.; Nakayama, H.; Ihara, H. *Chem. Lett.* **1999**, 1165.
(24) Ihara, H.; Yoshitake, M.; Takafuji, M.; Yamada, T.; Sagawa, T.; Hirayama, C. *Liq. Cryst.* **1999**, *26*, 1021.
(25) Hachisako, H.; Murata, Y.; Ihara, H. *J. Chem. Soc., Perkin Trans. 2* **1999**, 2569.

10.1021/la0255267 CCC: $22.00
Published on Web 06/07/2002

Chart 1. L-Glutamic Acid-Derived Compounds with Protoporphyrin IX (1) or Pyrene (2) Moieties

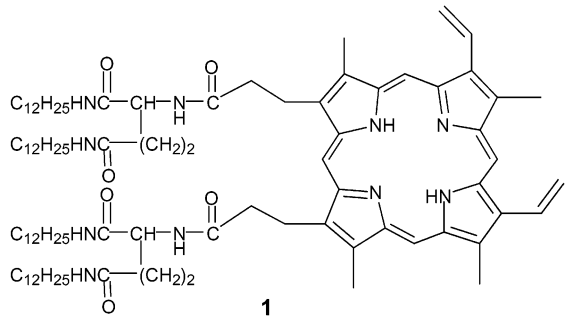

1

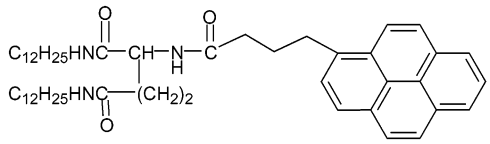

2

ization of labeled compounds. The objective of this study is to present the features of the photophysics of porphyrin and pyrene in the fibrous assemblies.

To mimic the structure and function of the photosynthetic antenna complex,[26] many organic chemists have reported porphyrin arrays by taking various kinds of strategies such as modification onto the solid surface, assembling along the stereoregular polymer {e.g., α-helical poly(α-amino acid)s}, and so on.[27−35] If we succeed in constructing the highly oriented assemblies of porphyrin- and pyrene-containing systems, these self-aggregation systems will be applicable to mimic the efficient energy transfer process in the photosynthetic antenna complex. The second purpose in this manuscript is to describe the preliminary results of steady-state fluorescence spectroscopic measurements to detect and enhance the singlet−singlet energy migration from pyrene to porphyrin in the mixed microfibrous assemblies.

Experimental Section

An L-glutamic acid derived compound with a porphyrin moiety (1) was synthesized by the amide linkage reaction of protoporphyrin IX with *N′*,*N′*-didodecyl L-glutamide. A 0.20 g portion (0.36 mmol) of protoporphyrin IX was dispersed in benzene (30 cm^3) and thionyl chloride (25 cm^3, 0.36 mol), and the mixture was refluxed for 6 h under stirring. The residue obtained by the solvent evaporation was dissolved in benzene (30 cm^3) and mixed with the solution of *N′*,*N′*-didodecyl-L-glutamide[26] (0.44 g, 0.92 mmol) in benzene (100 cm^3) containing 0.39 cm^3 (2.8 mmol) of triethylamine. The mixture was stirred for 1 day at 37 °C. After the separation of the precipitate (triethylamine hydrochloride) from the mixture, the filtrate was evaporated to dryness. The residue of the crude product was purified by chromatography on a silica gel column (Wako gel C-200) eluting with 20:1 chloroform/methanol. The first fraction was evaporated to dryness, and the residue was dissolved in benzene. The organic layer was washed two times with 0.2 N NaOH and 0.2 N HCl, respectively, washed with water, and dried with sodium sulfate. The solution was evaporated to dryness in vacuo to give a dark brown solid. FT-IR (KBr): 3390 (nNH), 1657 (amide I), and 1550 (amide II) cm^{-1}. MALDI-TOF (2,5-dihydroxybenzoic acid): $m/z = 1650$ ($M + H^+$); calcd for $C_{92}H_{148}N_{10}O_6 \cdot 9/2Cl$, 1649.[36] The NMR spectrum of **1** gives serious line-broadened proton signals. Elemental analysis calcd for $C_{92}H_{148}N_{10}O_6 \cdot 9/2Cl$: C, 67.0; H, 9.0; N, 8.5. Found: C, 66.8; H, 9.2; N, 7.5%.

A pyrene-containing didodecylamide-type compound (**2**) was prepared by the condensation of 1-pyrenebytyric acid (0.37 g, 1.3 mmol) and 0.60 g (1.2 mmol) of *N′*,*N′*-didodecyl-L-glutamide by using triethylamine (58 cm^3, 0.41 mol) and diethyl cyanophosphate (0.48 g, 0.45 mol) in $CHCl_3$ (70 cm^3). After being stirred for 1 day at room temperature, the solution was concentrated in vacuo. The residue was redissolved in chloroform, and the organic layer was washed three times with 0.2 N NaOH and 0.2 N HCl, respectively, washed with water, and dried with sodium sulfate. The solution was concentrated in vacuo, and the residue was recrystallized from methanol and dried in vacuo to give a pale yellow solid: yield, 0.89 g (93%). MALDI-TOF (2,5-dihydroxybenzoic acid): $m/z = 753$ ($M + H^+$); calcd for $C_{49}H_{73}N_3O_3$, 752. ^1H NMR ($CDCl_3$, 400 MHz): $\delta = 8.05$ (9H, m, pyrene), 7.05 (1H, br, NH), 6.81 (1H, br, NH), 5.96 (1H, br, NH), 4.34 (1H, d, −C*H−), 3.36 (2H, br, $-CH_{2-}$), 3.20 (2H, br, $-CH_2NHCO-$), 2.39 (2H, tr, $-CH_2CO-$), 2.24 (2H, t, $-CH_2CO-$), 1.93 (2H, q, $-CH_{2-}$), 1.46 (4H, br, $-CH_{2-}$), 1.21 {36H, br, $-(CH_2)_{9-}$}, 0.87 (6H, t, CH_3). Elemental analysis calcd for $C_{49}H_{73}N_3O_3$: C, 78.2; H, 9.8; N, 5.6. Found: C, 77.5; H, 9.6; N, 5.4%. mp: 190−195 °C.

Electron micrographs were obtained using a JEOL JSM-2000FX. UV−vis spectrophotometry and circular dichroism spectropolarimetry were carried out with a Hitachi U-2000 and a JASCO J-725, respectively. Fluorescence characterization was performed by using a JASCO FP-550A.

Results and Discussion

Transmission Electron Microscopic (TEM) Observation of Self-Assembled Fibrillar Networks As Found in Organic Media. Even at the concentration of 5.0 mmol dm^{-3} of the porphyrin-containing compound (**1**), the gelation was not visually observed in benzene, chloroform, ethanol, and so on at the temperature range from 10 to 60 °C. On the other hand, formation of organic gels of the pyrene-containing compound (**2**) can be visually observed in benzene or cyclohexane. It was found by the inverted tube method[37] at 25 °C that **2** formed organic gels in benzene at the concentration of more than 1.0 mmol dm^{-3}. TEM observation of **1** and **2** aggregates in the cast films from various benzene solutions showed a self-assembled and well-developed fibrous network as seen in Figure 1c−g. The diameters of these fibrous networks are around several tens to hundreds of nanometers although their detailed morphologies are different in their lengths and widths.

Their lengths will be at least in the order of hundreds of micrometers. For example, the geometric dimensions of **1** are 3.59 × 1.57 × 0.83 nm^3 estimated with CAChe-MM2 calculations. Therefore, we estimate that the minimum sizes of the fibrous aggregates of **1** and **2** are based on a multimolecule-layered structure at least. In

(26) McDermott, G.; Prince, S. M.; Freer, A. A.; Hawthornthwaite, A. M.; Papiz, M. Z.; Cogdell, R. J.; Isaacs, N. W. *Nature* **1995**, *374*, 517.
(27) Balzani, V.; Scandola, F. *Supramolecular Photochemistry*, 1st ed.; Ellis Horwood: New York, 1991.
(28) Schenning, A. P. H. J.; Benneker, F. B. G.; Geurts, H. P. M.; Liu, X. Y.; Nolte, R. J. M. *J. Am. Chem. Soc.* **1995**, *118*, 8549.
(29) Kondo, T.; Ito, T.; Nomura, S.; Uosaki, K. *Thin Solid Films* **1996**, *284*, 652.
(30) Mihara, H.; Tomizaki, K.; Fujimoto, T.; Sakamoto, S.; Aoyagi, H.; Nishino, N. *Chem. Lett.* **1996**, 187.
(31) Aoudia, M.; Rodgers, M. A. J. *J. Am. Chem. Soc.* **1997**, *119*, 12859.
(32) Anderson, H. L. *Chem. Commun.* **1999**, 2323.
(33) Schwab, P. F. H.; Levin, M. D.; Michl, J. *Chem. Rev.* **1999**, *99*, 1863.
(34) Imahori, H.; Nishimura, Y.; Norieda, H.; Karita, H.; Yamazaki, I.; Sakata, Y.; Fukuzumi, S. *Chem. Commun.* **2000**, 661.
(35) Ikeda, M.; Sugasaki, A.; Kubo, Y.; Sugiyasu, K.; Takeuchi, M.; Shinkai, S. *Chem. Lett.* **2001**, 1266.

(36) There are nine peaks at regular mass intervals of 34 (= Cl) in the mass spectrum of **1** as shown in the Supporting Information available. The average measured mass (five data sets) which is located in the center of nine peaks is 1650. This value of mass is larger by 159 than the theoretical molecular weight of $C_{92}H_{148}N_{10}O_6$ (1490) as shown in Chart 1, ascribed to the presence of 9/2Cl.

(37) Lin, Y. C.; Kacher, B.; Weiss, R. G. *J. Am. Chem. Soc.* **1989**, *111*, 5542.

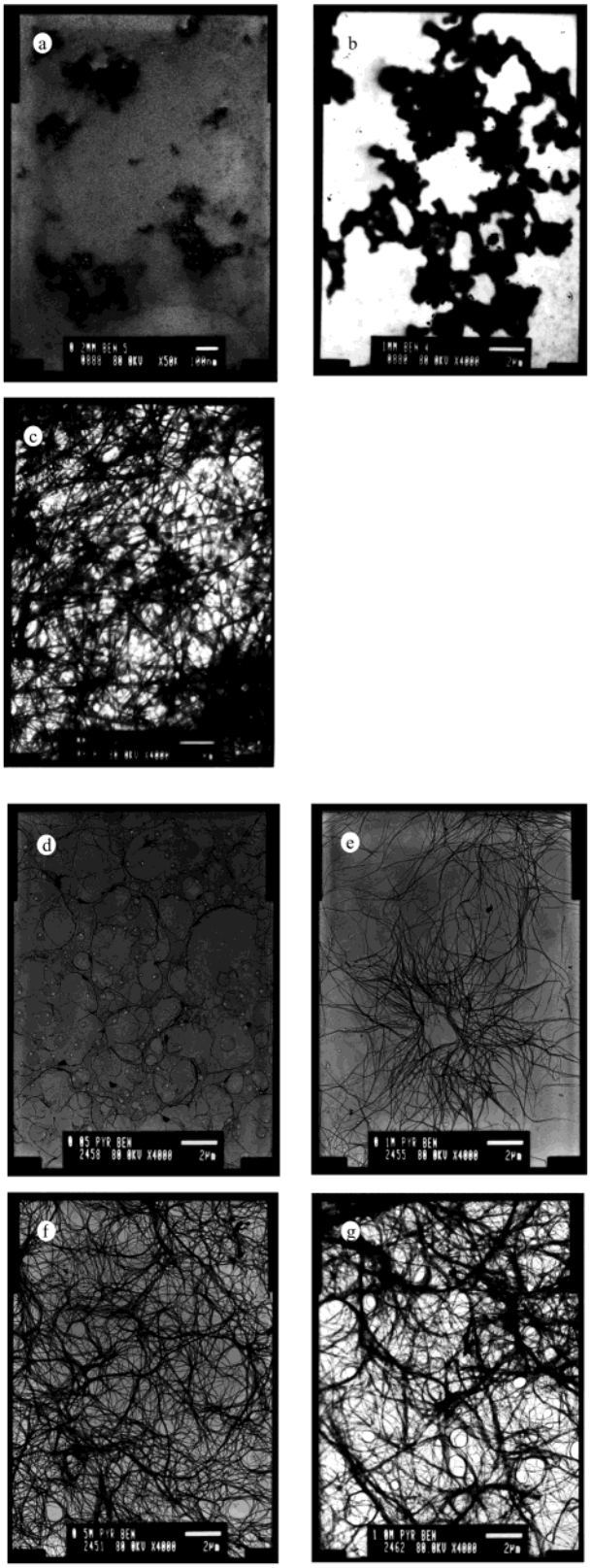

Figure 1. TEM images of **1** {(a) 0.2 mmol dm^{-3}, (b) 1.0 mmol dm^{-3}, and (c) 5.0 mmol dm^{-3}} and **2** {(d) 0.05 mmol dm^{-3}, (e) 0.10 mmol dm^{-3}, (f) 0.50 mmol dm^{-3}, and (g) 1.0 mmol dm^{-3}} aggregates in the cast films from benzene solutions. Stained by 2 wt % ammonium molybdate.

contrast, small amounts of aggregated particles prior to the fibrous network were seen in Figure 1a,b.

Porphyrin-Containing System. Porphyrin incorporated in the microfibrous assemblies would act in the role of a probe to characterize its self-assembling behavior. As

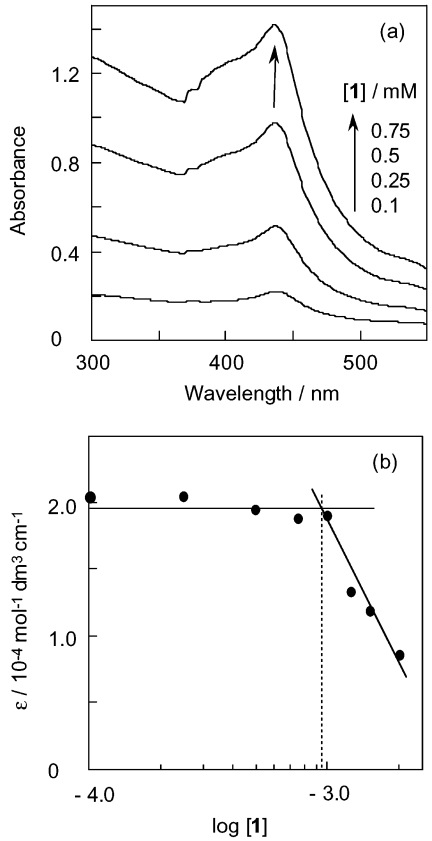

Figure 2. UV−vis spectra (a) and the molecular coefficient (e) at 436 nm (b) of **1** in benzene at 25 °C.

shown in Figure 2a, visible spectra of **1** in benzene at 25 °C show a Soret peak at 436 nm which is blue-shifted from 460 nm, assigned to be a Soret peak of the monomeric dispersion state of the original protoporphyrin IX. The blue shift of the Soret band implies that the porphyrin rings in the fibrous assemblies are stacked according to the H-aggregation mode.[38] The plots of the molecular coefficient at 436 nm (ϵ_{436}) versus log [**1**] (Figure 2b) showed that ϵ_{436} decreased remarkably at the concentrations over 1.0 mmol dm^{-3}.

On the other hand, the CD spectra showed a positive Cotton effect (induced CD) with molar ellipticity {+1850° cm^2 dmol^{-1} at 425 nm (θ_{425})} as shown in Figure 3. The plot of θ_{425} versus log [**1**] (Figure 3b) shows that θ_{425} increased remarkably at the concentrations over 1.0 mmol dm^{-3}.

We consider that the increase of θ_{425} (or the decrease of the Soret peak at 436 nm) is not related to the gel formation but indicates microenvironmental change such as highly oriented aggregation. The critical point (concentration) in Figure 2b and Figure 3b will be attributable to the cac of **1** in benzene. Therefore, the concentrations over 1.0 mmol dm^{-3} are brought about through the network with development of the fibrous aggregates. Different TEM images in Figure 1a−c described above support this. It is also proved that **1** can form highly oriented aggregates even at the sol-forming concentration.

Figure 4 shows the visible spectra at various temperatures. The Soret peak at 436 nm decreased with lowering the temperature from 60 to 15 °C, while the CD intensity at 425 nm increased with lowering the temperature from 60 to 25 °C as shown in Figure 5.

(38) Kasha, M.; Rawls, H. R.; El Bayuomi, M. A. E. *Pure Appl. Chem.* **1965**, *11*, 371.

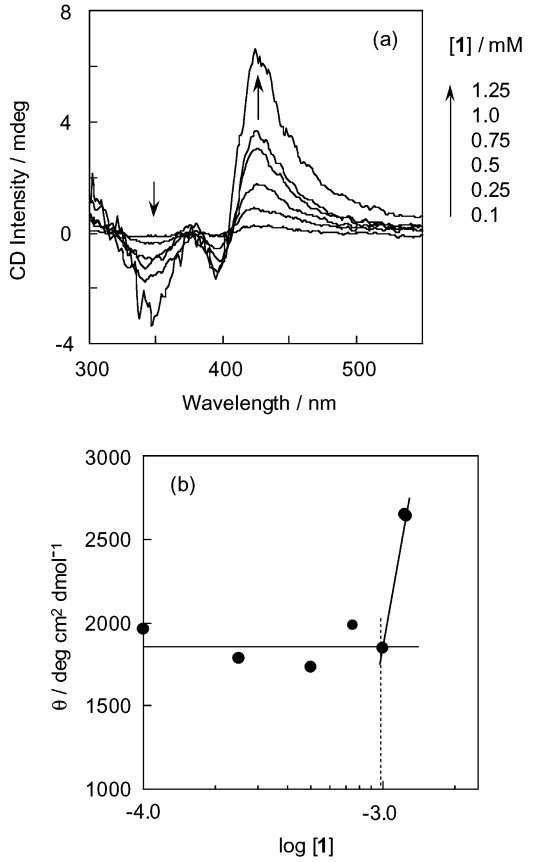

Figure 3. CD spectra (a) and molar ellipticity (θ) at 425 nm (b) of **1** in benzene at 25 °C.

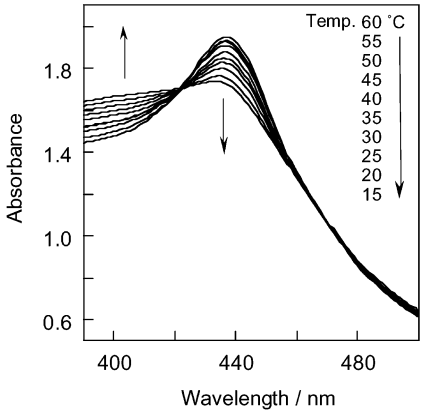

Figure 4. Temperature dependence of the visible spectra of **1** (1.0 mmol dm^{-3}) in benzene using a 1 mm quartz cell.

This indicates that highly oriented network structures were formed at low temperature, and thus the temperature affects the features of the photophysics of porphyrin in the microfibrous assemblies.

We previously discussed the driving force for aggregation of the L-glutamic acid derived systems:[18−25] the three amide moieties around the L-glutamic acid parts can act as hydrogen bonding interaction sources for formation of the network. In this respect, when trifluoroacetic acid as an inhibitor of hydrogen bonding interactions was added to the benzene solution of 1, there were remarkable visible and CD spectral changes: a red shift of the Soret peak from 436 to 460 nm and a remarkable decrease of optical activity (Figure 6 and Figure 7).

According to the results of these observations, we propose that the self-assemblies of **1** are the cofacial packed-porphyrin planes aggregated due to the hydrogen bonding through the six amide bondings of the L-glutamic acid−dialkyl moiety of **1**.

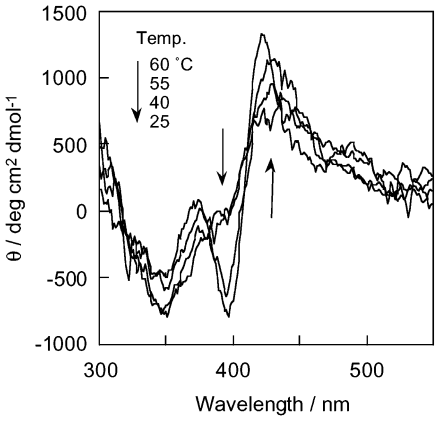

Figure 5. Temperature dependence of the CD spectra of **1** (1.0 mmol dm^{-3}) in benzene using a 1 mm quartz cell.

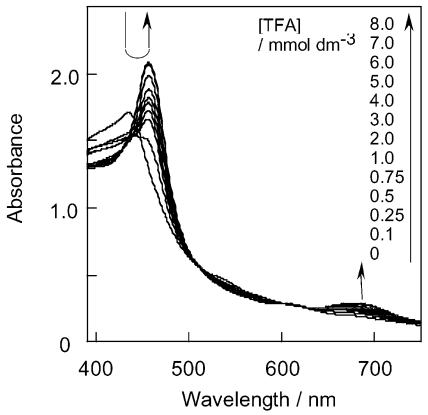

Figure 6. Visible spectral changes caused by the addition of trifluoroacetic acid (0−8.0 mmol dm^{-3}) to **1** (1.0 mmol dm^{-3}) in benzene at 25 °C using a 1 mm quartz cell.

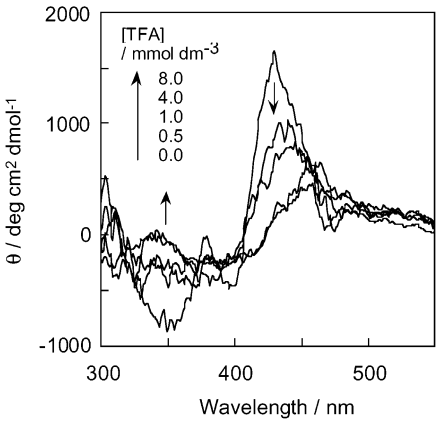

Figure 7. CD spectral changes caused by addition of trifluoroacetic acid (0−8.0 mmol dm^{-3}) to **1** (1.0 mmol dm^{-3}) in benzene at 25 °C using a 1 mm quartz cell.

Pyrene-Containing System. Figure 8 shows the UV absorption spectra of **2** in benzene at various concentrations. The electronic transition of pyrene is likely to be ^1L_a (allowed) at 346 nm; there is a transition at a longer wavelength (^1L_b).[39] When the concentration of **2** increases, the broadening of the absorption bands is accompanied by a decrease of the extinction coefficients (Figure 9), while drastic CD spectral changes of **2** were observed in benzene at various concentrations as seen in Figure 10.

(39) Winnik, F. M. *Chem. Rev.* **1993**, *93*, 587.

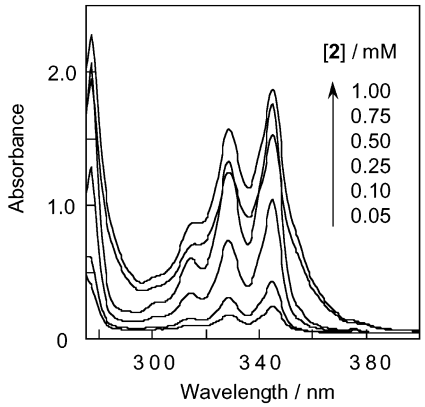

Figure 8. UV absorption spectra of **2** in benzene at 25 °C.

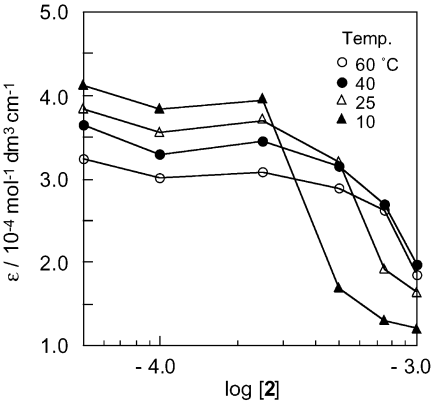

Figure 9. Molecular coefficient (ϵ) at 346 nm of **2** in benzene.

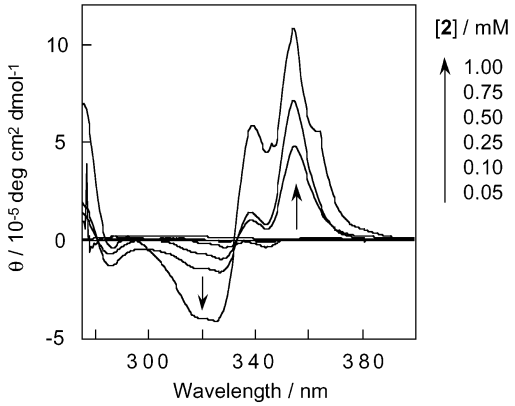

Figure 10. CD spectra of **2** in benzene at 25 °C.

Figure 11 (or Figure 9) showed that θ_{368} increased (or ϵ_{346} decreased) remarkably at the concentrations over 0.25 mmol dm^{-3}. Although the TEM observations in Figure 1d−g indicate the formation and development of microfibrous networks, **2** did not produce a gel state at the concentration of 0.5 mmol dm^{-3} at 25 °C. Therefore, these critical points are not related to the gel formation but indicate microenvironmental change such as highly oriented aggregation similar to the case of **1**. In this sense, the pyrene moiety can play the role of a probe to characterize its highly oriented self-assembling behavior.

The temperature dependence of UV absorption and CD spectra are also summarized in Figures 9 and 11. The ϵ_{346} decreased with lowering the temperature (Figure 9), and the θ_{368} increased drastically at the temperatures below 25 °C (Figure 11). According to these spectroscopic observations of **2** at various temperatures, the temperature also affects transformation of the self-assembled state of

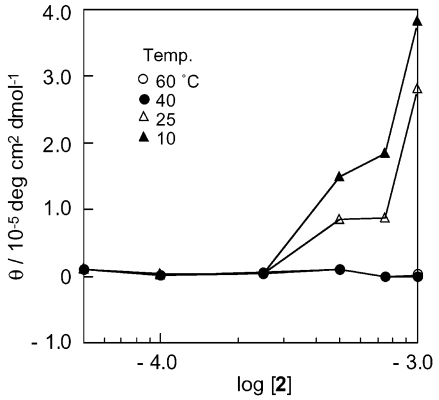

Figure 11. Molar ellipticity (θ) at 368 nm of **2** in benzene.

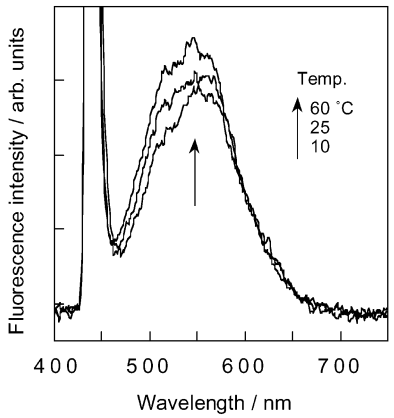

Figure 12. Fluorescence spectra of **1** (0.1 mmol dm^{-3}) in benzene at 10, 25, and 60 °C with excitation at 436 nm.

2 and the properties of the photophysics of pyrene in the microfibrous aggregates.

Steady-State Emission Spectra of Porphyrin and/or Pyrene-Containing Systems. The steady-state emission of **1** in benzene was measured with the excitation wavelength at 436 nm (Figure 12). The emission did not vary remarkably by changing the temperature.

In contrast, it is known that the monomer fluorescence of pyrene is very sensitive to its surroundings.[40] This effect is also expected in our case by measuring the fluorescence emission of the pyrene-containing system. When **2** was dissolved in benzene at 25, 40, or 60 °C, the emission band was observed at 381 nm. This band is assigned to be the monomer fluorescence of a pyrene moiety. This implies that compound **2** disperses as a monomeric state at 25−60 °C. Upon cooling to 10 °C, new bands centered at 420 nm (E_1) and 450 nm (E_2) are observed, and these are assigned to be the excimer formation[39,41] as seen in Figure 13.

The monomer-to-excimer transition was also concentration dependent as shown in Figure 14. Although the concentration quenching of the excimers was observed, excimer emission, relative to the monomer emission, increases as the amount of **2** increases. Therefore, the excimer formation may be closely related to the highly oriented self-assembling of **2**.

The excimer emission of **2** in Figures 13 and 14 overlaps well with the absorption of **1** in Figure 2a. Thus, it is expected that excitation of the pyrene moiety as an antenna chromophore may lead to efficient singlet−singlet

(40) Nakajima, A. *Bull. Chem. Soc. Jpn.* **1971**, *44*, 3272.
(41) Birks, J. B. *Photophysics and Photochemistry*; Cambridge University Press: Cambridge, 1985; p 141.

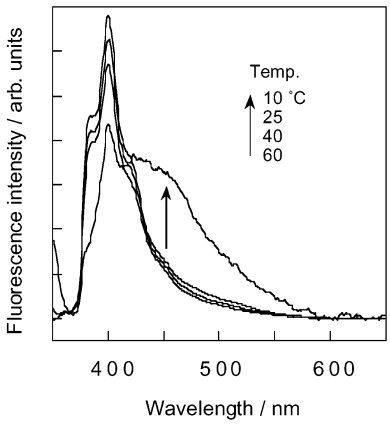

Figure 13. Temperature dependence of fluorescence spectra of **2** (0.50 mmol dm^{-3}) in benzene with excitation at 350 nm.

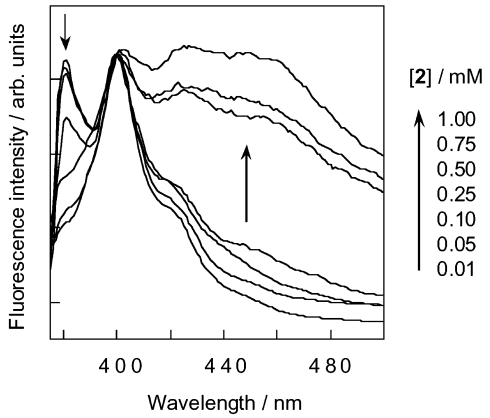

Figure 14. Fluorescence spectra of **2** in benzene at 10 °C with excitation at 350 nm.

Chart 2. Energy Transfer from the Excimer−Pyrene Complex to the Ground-State Free Base Porphyrin

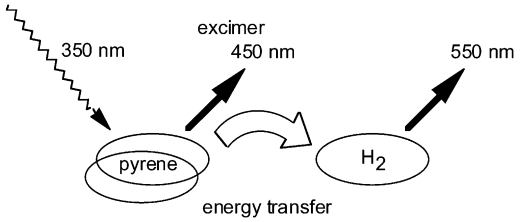

energy migration from the pyrene to the porphyrin in highly oriented and self-assembling networks as shown in Chart 2.

Fluorescence spectra at various concentration ratios of [**2**]/[**1**] from 1 to 10 at various temperatures from 10 to 60 °C have been measured. When the ratio of [**2**]/[**1**] was 4, a weak emission was observed at 550 nm as shown in Figure 15a, and the emission intensities gradually increased with lowering the temperature from 60 to 10 °C. These emission intensities also increased with increasing the [**2**]/[**1**] ratio from 4 to 10 (Figure 15b). This result under these critical conditions is attributable to the remarkable enhancement of the excimer formation of **2**.

Although a precise evaluation of intrinsic quantum yield for energy transfer is not clear-cut, at least, energy transfer from the excimer−pyrene complex to the ground-state free base porphyrin was realized under steady-state irradiation by the enhancement of the excimer emission of **2** through the highly oriented and self-assembling structures.

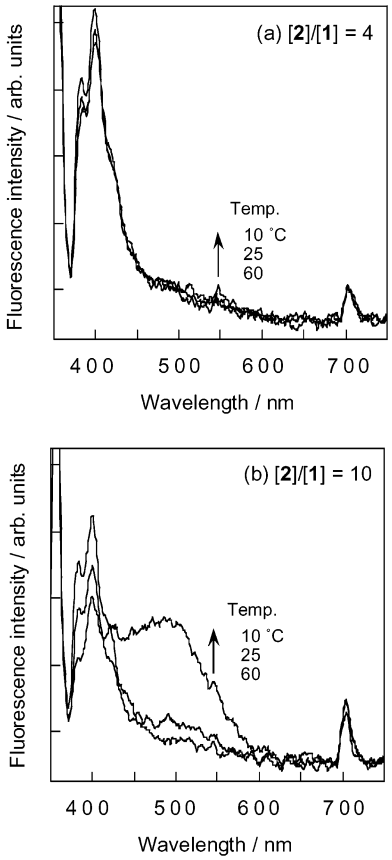

Figure 15. Fluorescence spectra of a mixed system of **1** (0.1 mmol dm^{-3}) and **2** {0.4 mmol dm^{-3} (a) or 1.0 mmol dm^{-3} (b)} in benzene at 10, 25, and 60 °C with excitation at 350 nm.

Conclusion

Porphyrin and pyrene substituted by dialkyl L-glutamic acid compounds make fibrillar networks in benzene. Chromophoric probes of porphyrin and pyrene moieties enable evaluation of their assembling behavior photophysically even at a low concentration below the critical gel concentration through UV−vis, CD, and fluorescence spectroscopic characterization. Experimental results showed the correspondence to each other, and the spectroscopic characterizations were able to compensate the lack of TEM observation for the aggregation in the dilute solution. In particular, we have obtained the preliminary results of fluorescence spectra regarding the singlet−singlet energy migration taking place from the excimer−pyrene complex to the ground-state free base porphyrin in the mixed assemblies for mimicry of the efficient energy transfer process of the photosynthetic antenna complex.

Acknowledgment. This research was supported in part by a Grant-in-Aid for Scientific Research (#10680572, H.I.) from the Ministry of Education, Science, Sports, and Culture of Japan.

Supporting Information Available: MALDI-TOF MS spectrum of **1**. CPK model conformation of **1** estimated by molecular mechanics calculations with CAChe-MM2. This material is available free of charge via the Internet at http://pubs.acs.org.

LA0255267